

Electronic Supplementary Information (ESI)

1. BADER charge analysis

Table S1. Effective electronic charge on constituent atoms within a molecule by Bader charge analysis.

2D nanomaterial		Charge on different atoms (in electronic charge unit)		
		M	X	X (for pristine) or Y (for Janus)
Pristine	GeS ₂	+1.306	-0.652	-0.654
	GeSe ₂	+0.927	-0.464	-0.463
	SnS ₂	+1.529	-0.763	-0.766
	SnSe ₂	+1.227	-0.614	-0.613
	HfS ₂	+2.076	-1.038	-1.038
Janus	GeSSe	+1.114	-0.479	-0.635
	SnSSe	+1.379	-0.625	-0.754
	ZrSSe	+1.976	-0.914	-1.062

The Janus GeSSe (MXY) monolayer can be constructed from pristine GeSe₂ (MX₂) monolayer as it confirms an energetically favorable process. Therefore, by convention M, X and Y stands for Ge, Se and S respectively. (Calculation of BADER charge for ZrSSe monolayer has been done to compare/benchmark our findings against published results.¹)

2. Lattice Dynamical Stability

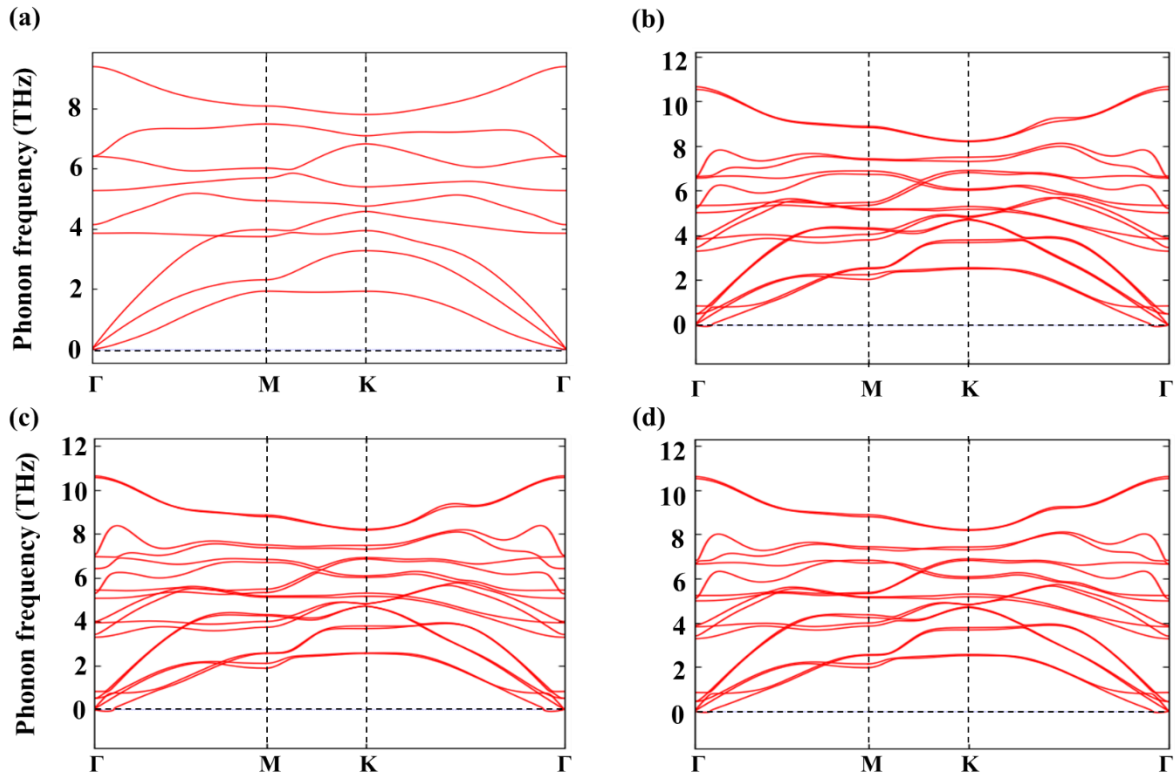


Fig. S1. Phonon dispersion of Janus (a) SnSSe monolayer; and GeSSe bilayer of (b) stacking-I, (c) stacking-II and (d) stacking-III.

Here dynamical stabilities of Janus SnSSe monolayer and GeSSe bilayer (stacking-I, II, III) have been studied by phonon dispersion, calculated using finite displacement method (FDM) as implemented in VASP and post-processed by Phonopy code. Using $7 \times 7 \times 1$ supercell dimension with $3 \times 3 \times 1$ k-points sampling, Janus SnSSe monolayer shows no imaginary frequency, as shown in Fig. S1 (a). While for the GeSSe bilayer system, we have used $6 \times 6 \times 1$ supercell dimension with $3 \times 3 \times 1$ k-points sampling, to take into account of the increase in the number of atoms in the unit cell, therefore computational time. Apart from a very small pocket of negative frequency (negligibly -0.06 , -0.09 and -0.07 THz for stacking I, II, III respectively) near the Gamma (Γ) point, no negative frequencies were observed in the entire 1st Brillouin zone (BZ) for Janus GeSSe bilayer, as presented in Fig. S1 (b), (c) and (d). The small pocket of phonon instability is extremely sensitive to the supercell size and k -point sampling, therefore ceases to be zero with larger supercell size, which is computationally expensive. Moreover, the magnitudes of negative frequencies are very close to zero and it changes by the amount by which the acoustic branches (LA) of dispersion curve miss zero when Newton's third law is not imposed on the matrix of the force constants.³

Also, a small structural instability in the flexural acoustic (ZA) modes around the Γ point was found for the well-studied graphene, silicene, molybdenum disulfide and gallium chalcogenides.³ It simply indicates the difficulty in achieving numerical convergence for ZA mode via first-principles calculations in 2D materials. Consequently, no appreciable imaginary vibrational frequency suggests that the Janus monolayer GeSSe and SnSSe along with Janus bilayer GeSSe (stacking I, II and III) are dynamically stable.

3. Electronic Properties of Pristine and Janus Monolayer

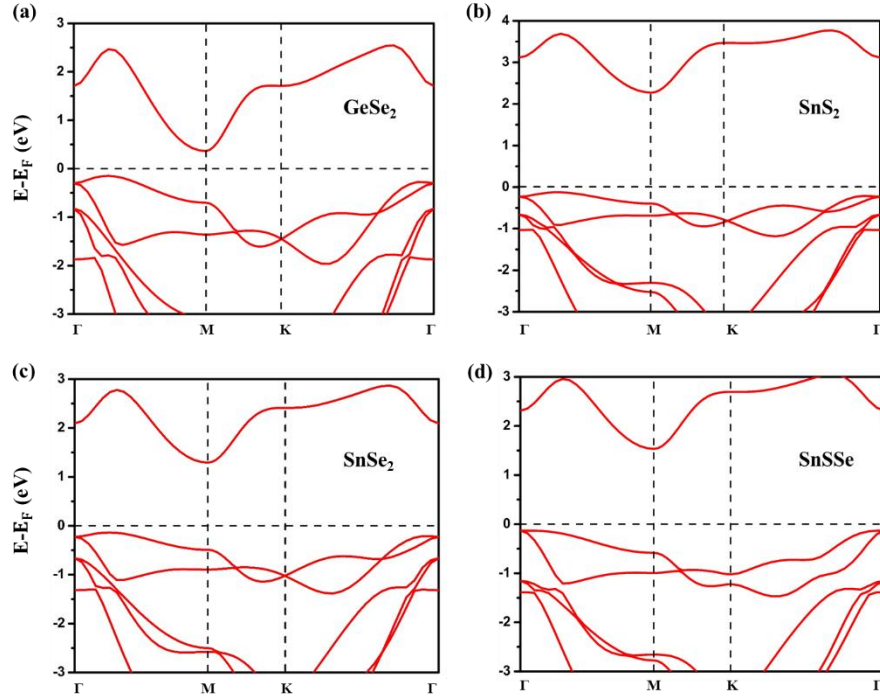


Fig. S2. Electronic band structure (HSE06) of (a) GeSe₂ (b) SnS₂ (c) SnSe₂ and (d) SnSSe monolayer (taking Fermi energy as 0 eV reference).

It has been found that for pristine GeS₂, GeSe₂, SnS₂, SnSe₂ monolayers and Janus GeSSe monolayer (as well as bilayer), the conduction band minimum (CBM) occurs at the M point and the valence band maximum (VBM) arise between Γ to M points (inclined towards the Γ point) of the BZ, illuminating indirect bandgap nature. But for Janus SnSSe monolayer, the CBM occurs at the M point and the (VBM) arise at the Γ point of the BZ, therefore also illuminating indirect bandgap nature.

4. Piezoelectric property

From main text [equation (9)], the relation between piezoelectric stress and strain coefficient is

$$e_{il} = d_{ip} C_{pl} \quad (S1)$$

where the dummy index p runs from 1 to 6 while $i, l = 1, 2, 3$

The above equation has been solved numerically to calculate d_{ip} matrix (3x6) based on the e_{il} matrix (3x6) and C_{pl} matrix (6x6).

For unstrained condition, the two non-zero piezoelectric strain coefficients, i.e., d_{22} and d_{31} , can be expressed in a simplified form of equation (S1), as:

$$d_{22} = \frac{e_{22}}{C_{11}-C_{12}}$$

$$d_{31} = \frac{e_{31}}{C_{11}+C_{12}} \quad (S2)$$

Now, for strained system, where $C_{11} \neq C_{22}$ (except for isotropic biaxial strain), a generalized form has been used to determine piezoelectric strain coefficients by incorporating anisotropy in elastic constant coefficients, given as:

$$d_{22} = \frac{C_{11}e_{22}-C_{12}e_{21}}{C_{11}C_{22}-C_{12}^2}$$

$$d_{31} = \frac{C_{22}e_{31}-C_{12}e_{32}}{C_{11}C_{22}-C_{12}^2} \quad (S3)$$

Equations (S2) and (S3) are the analytically simplified form of equation (S1). The deduction is provided below. The equation (S3) is applicable for both strained and unstrained systems. Also, the results obtained from the direct solution to equation (S1) and from the simplified equations (S3) are close enough.

4.1. Deduction/derivation of equation:

(a) From equation (S1), $e_{il} = d_{ip}C_{pl}$ (where dummy index, p varies from 1 to 6), we can get,

$$e_{21} = d_{21}C_{11} + d_{22}C_{21} + d_{23}C_{31} + d_{24}C_{41} + d_{25}C_{51} + d_{26}C_{61} \quad (S4)$$

At strained (as well as unstrained) condition of Janus MXY monolayer, elastic constant coefficients, $C_{31} \rightarrow 0$, $C_{41} \rightarrow 0$, $C_{51} \rightarrow 0$ and $C_{61} \rightarrow 0$. Therefore, equation (S4) reduces to

$$e_{21} = d_{21}C_{11} + d_{22}C_{21} \quad (S5)$$

Again from equation (S1), we can get,

$$e_{22} = d_{21}C_{12} + d_{22}C_{22} + d_{23}C_{32} + d_{24}C_{42} + d_{25}C_{52} + d_{26}C_{62} \quad (S6)$$

Also, at strained (as well as unstrained) condition of Janus MXY monolayer, elastic constant coefficients $C_{32} \rightarrow 0$, $C_{42} \rightarrow 0$, $C_{52} \rightarrow 0$ and $C_{62} \rightarrow 0$. Therefore, equation (S6) reduces to

$$e_{22} = d_{21}C_{12} + d_{22}C_{22} \quad (S7)$$

(S5) $\times C_{12}$ - (S7) $\times C_{11}$ gives, $C_{12}e_{21} - C_{11}e_{21} = d_{22} (C_{12}^2 - C_{11}C_{22})$

$$d_{22} = \frac{C_{11}e_{22}-C_{12}e_{21}}{C_{11}C_{22}-C_{12}^2}$$

(b) In a similar manner, from equation (S1), we can get,

$$e_{31} = d_{31}C_{11} + d_{32}C_{21} + d_{33}C_{31} + d_{34}C_{41} + d_{35}C_{51} + d_{36}C_{61} \quad (S8)$$

At strained (as well as unstrained) condition of Janus MXY monolayer, elastic constant coefficients $C_{31} \rightarrow 0$, $C_{41} \rightarrow 0$, $C_{51} \rightarrow 0$ and $C_{61} \rightarrow 0$. Therefore, equation (S8) reduces to

$$e_{31} = d_{31}C_{11} + d_{32}C_{21} \quad (\text{S9})$$

Again from equation (S1), we can get,

$$e_{32} = d_{31}C_{12} + d_{32}C_{22} + d_{33}C_{32} + d_{34}C_{42} + d_{35}C_{52} + d_{36}C_{62} \quad (\text{S10})$$

Also, at strained (as well as unstrained) condition of Janus MXY monolayer, elastic constant coefficients $C_{32} \rightarrow 0$, $C_{42} \rightarrow 0$, $C_{52} \rightarrow 0$ and $C_{62} \rightarrow 0$. Therefore, equation (S10) reduces to

$$e_{32} = d_{31}C_{12} + d_{32}C_{22} \quad (\text{S11})$$

(S9) $\times C_{22}$ - (S11) $\times C_{21}$ gives, $C_{22}e_{31} - C_{21}e_{32} = d_{31}(C_{11}C_{22} - C_{12}^2)$

$$d_{31} = \frac{C_{22}e_{31} - C_{12}e_{32}}{C_{11}C_{22} - C_{12}^2}$$

where both for strained and unstrained conditions, $C_{12} = C_{21}$.

These boxed equations are generalized form of in-plane (d_{22}) and out-of-plane (d_{31}) piezoelectric strain coefficient under the application of strain for given C_{3v} symmetry. For unstrained condition,

$$e_{22} = -e_{21},$$

$$e_{31} = e_{32},$$

$$\text{and } C_{11} = C_{22},$$

thus, generalized equations (S3) for d_{22} and d_{31} reduces to special equations (S2).

4.2. Lattice dynamical stability of strained Janus GeSSe monolayer:

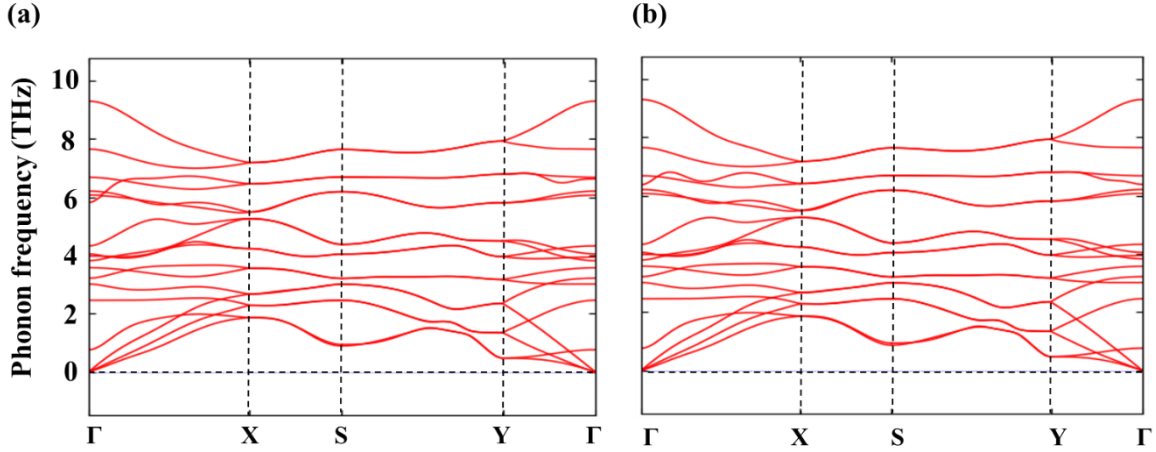


Fig. S3. Phonon dispersion of Janus GeSSe monolayer under (a) 7% uniaxial tensile strain along arm-chair direction and (b) 7% biaxial tensile strain.

Absence of imaginary vibrational frequency implies dynamic stability in the Janus GeSSe monolayer under 7% uniaxial strain along arm-chair direction and 7% biaxial strain. Also, in this strained condition, Janus GeSSe monolayer is found to be mechanically stable. Therefore, both dynamical and mechanical stability has been ascertained under aforementioned strained condition.

4.3. Enhancement of piezoelectricity under strain in Janus GeSSe monolayer:

- Under the application of uniaxial and biaxial strain in Janus GeSSe monolayer, the results have been summarized below.

Table S2. Calculated parameters: piezoelectric strain coefficients, d_{ij} (pm/V); HSE06 bandgap, E_g (eV) and induced basal-plane pressure (GPa) of Janus GeSSe monolayer at different strain.

Strained GeSSe ML	d_{22}	d_{31}	d_{33}	d_{15}	E_g	Pressure
0% or unstrained	4.09	0.15	0.59	7.90	0.75	0.00
7% uniaxial_ AC	267.07	1.35	5.16	702.34	0.65	-1.03
7% biaxial	68.04	0.22	4.70	178.36	1.13	-1.89

- Under the application of uniaxial and biaxial strain on Janus GeSSe monolayer, the variation in bandgap and layer thickness have been shown below.

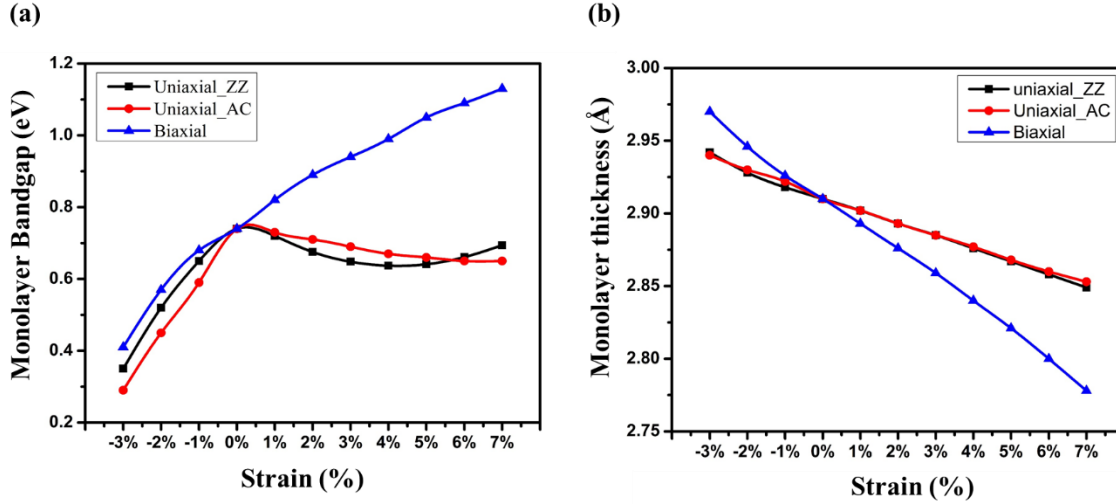


Figure S4. (a) Variation in bandgap and (b) layer thickness for strained Janus GeSSe monolayer.

4.4. Mechanical stability of strained Janus GeSSe monolayer under uniaxial zig-zag strain:

When the supercell is taken orthorhombic, then anisotropy comes into picture as $C_{11} \neq C_{22}$ anymore. Same criteria are applicable for strained system as there arises two different values of Young's modulus along two non-equivalent Cartesian [10] and [01] directions:

$$Y_{[10]}^{2D} = \frac{C_{11}^2 - C_{12}^2}{C_{22}} \quad \text{and} \quad Y_{[01]}^{2D} = \frac{C_{11}^2 - C_{12}^2}{C_{11}}$$

As a result, two different values of Poisson's ratio will arise:

$$\nu_{[10]}^{2D} = \frac{C_{12}}{C_{22}} \quad \text{and} \quad \nu_{[01]}^{2D} = \frac{C_{12}}{C_{11}}$$

The pictorial representation of mechanical stability of Janus GeSSe monolayer under the application of uniaxial strain along zig-zag direction has been shown in Fig S4. It is clearly observable that $(C_{11} - C_{12}) > 0$ and $(C_{22} - C_{12}) > 0$ is being satisfied till 10% uniaxial zig-zag strain. Therefore, the Janus GeSSe monolayer is mechanically stable, as per the satisfaction of Born-Huang stability criteria, under above mentioned strain.

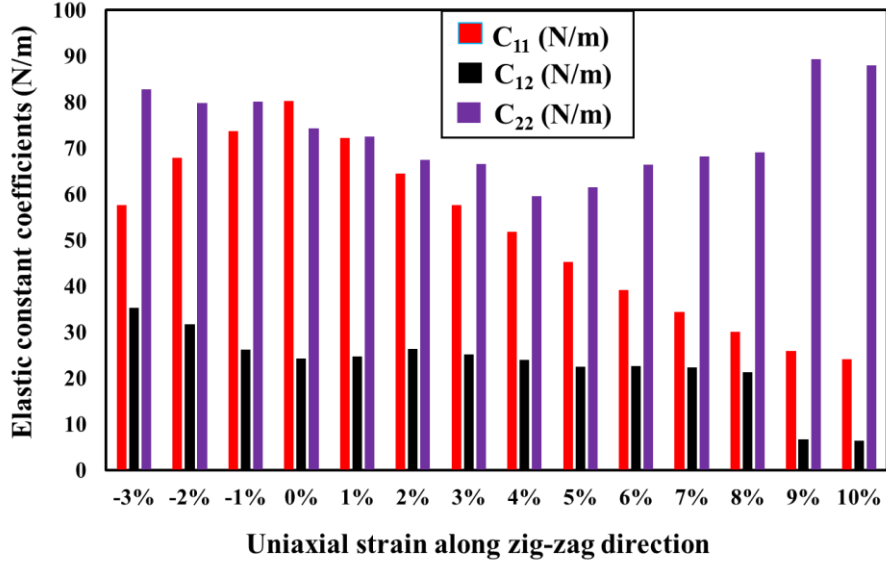


Figure S5. Variation of in-plane elastic constant coefficients C_{11} , C_{12} and C_{22} (N/m) with uniaxial strain along the zig-zag direction for Janus GeSSe monolayer.

5. Carrier Mobility

$$\mu_{\alpha_y} \approx \frac{e\hbar^3 \left(\frac{5C_{y2D} + 3C_{x2D}}{8} \right)}{k_B T (m_{\alpha y})^{\frac{3}{2}} (m_{\alpha x})^{\frac{1}{2}} \left(\frac{9E_{\alpha y}^2 + 7E_{\alpha y}E_{\alpha x} + 4E_{\alpha x}^2}{20} \right)} 10^4 \text{ cm}^2 \text{V}^{-1} \text{s}^{-1} \quad (\text{S12})$$

The above equation gives the mobility of charge carrier along arm-chair direction (y) by Lang formalism. It can be achieved by interchanging x and y in equation (15) of the manuscript.

To calculate the value of deformation potential (DP), slope of linear fit to the variation in CBM (for electron) and VBM (for hole) with the application of infinitesimal uniaxial strain has been considered.

As we are interested only in the value of slope or variation in energy but not in the actual value of energy, the computationally inexpensive GGA-PBE exchange correlation functional has been employed to obtain the deformation potential from the variation in CBM and VBM with infinitesimal strain.

$$\mu_{\alpha_x} = \frac{e\hbar^3 3C_{x2D}}{k_B T m_{\alpha x} E_{\alpha x}^2} 10^4 \text{ cm}^2 \text{V}^{-1} \text{s}^{-1} \quad \mu_{\alpha_y} = \frac{e\hbar^3 3C_{y2D}}{k_B T m_{\alpha y} E_{\alpha y}^2} 10^4 \text{ cm}^2 \text{V}^{-1} \text{s}^{-1} \quad (\text{S13})$$

Equation (S13) is the original formulation of Bardeen and Shockley, where the carrier mobility, μ is independent of the sign of DP, i.e., $E_{\alpha x}$ and $E_{\alpha y}$. To be consistent with (S13), the magnitude of DP may only be entered in the equation (S12). $9E_{\alpha y}^2 + 7E_{\alpha y}E_{\alpha x} + 4E_{\alpha x}^2 = X$ occurs in the denominator of eqn. (S12). If $E_{\alpha y}$ and $E_{\alpha x}$ are of opposite sign, their product $E_{\alpha y}E_{\alpha x}$ can be negative. For certain values of $E_{\alpha y}$ and $E_{\alpha x}$, X can be negative. Then, the carrier mobility μ will be negative. However, μ is a physically

measurable quantity and hence, $\mu \geq 0$. In order to ensure $\mu \geq 0$, the modulus or the magnitude of $E_{\alpha y}$ and $E_{\alpha x}$ needs to be entered in eqn (S12) for a proper estimate of μ . Besides, the magnitude of deformation potential is typically entered by the scientific community in the calculation of carrier mobility.

The opposite signs in $E_{\alpha x}$ and $E_{\alpha y}$ cause an overestimation of carrier mobility in this work, as discussed below.

Table S3 (a) Calculated carrier mobility by Lang formulation 1, μ_{L_1} (with sign of DP); Lang formulation 2 μ_{L_2} (without sign of DP); Bardeen-Shockley (BS) formulation, μ_{BS} and piezoelectric scattering limited carrier mobility, μ_{PZ} , along zig-zag (x) and arm-chair (y) direction. All μ values are given in unit of $\text{cm}^2\text{V}^{-1}\text{s}^{-1}$.

Carrier	$\mu_{L_1_{\alpha x}}$	$\mu_{L_1_{\alpha y}}$	$\mu_{L_2_{\alpha x}}$	$\mu_{L_2_{\alpha y}}$	$\mu_{BS_{\alpha x}}$	$\mu_{BS_{\alpha y}}$	$\mu_{PZ_{\alpha x}}$	$\mu_{PZ_{\alpha y}}$
electron	2328	204	947	132	3928	74	13099	1368
hole	5962	480	1587	175	2023	144	3972	224

Table S3 (b) Calculated carrier mobility by Lang formulation 1, μ_{L_1} (with sign of DP); Lang formulation 2, μ_{L_2} (without sign of DP); Bardeen-Shockley (BS) formulation, μ_{BS} upon the incorporation of piezoelectric scattering limited carrier mobility μ_{PZ} , along zig-zag (x) and arm-chair (y) direction. All μ values are given in unit of $\text{cm}^2\text{V}^{-1}\text{s}^{-1}$.

Note that the LA and PZ mobilities (μ_{LA} & μ_{PZ}) have been added as per Matthiessen rule

Carrier	$\mu_{LA_1_{\alpha x} + P.Z.}$	$\mu_{LA_1_{\alpha y} + P.Z.}$	$\mu_{LA_2_{\alpha x} + P.Z.}$	$\mu_{LA_2_{\alpha y} + P.Z.}$	$\mu_{BS_{\alpha x} + P.Z.}$	$\mu_{BS_{\alpha y} + P.Z.}$
electron	1976	177	883	120	3021	71
hole	2384	153	1134	98	1340	87

where

$\mu_{L_1_{\alpha x}}$ = carrier mobility by Lang formulation 1 (with sign of DP)

$\mu_{L_2_{\alpha x}}$ = carrier mobility by Lang formulation 2 (without sign of DP)

$\mu_{BS_{\alpha x}}$ = carrier mobility as per Bardeen-Shockley formalism

$\mu_{PZ_{\alpha x}}$ = piezoelectric scattering limited carrier mobility

P.Z. = Piezoelectric Scattering

6. Janus GeSSe Bilayer

6.1 Electronic properties:

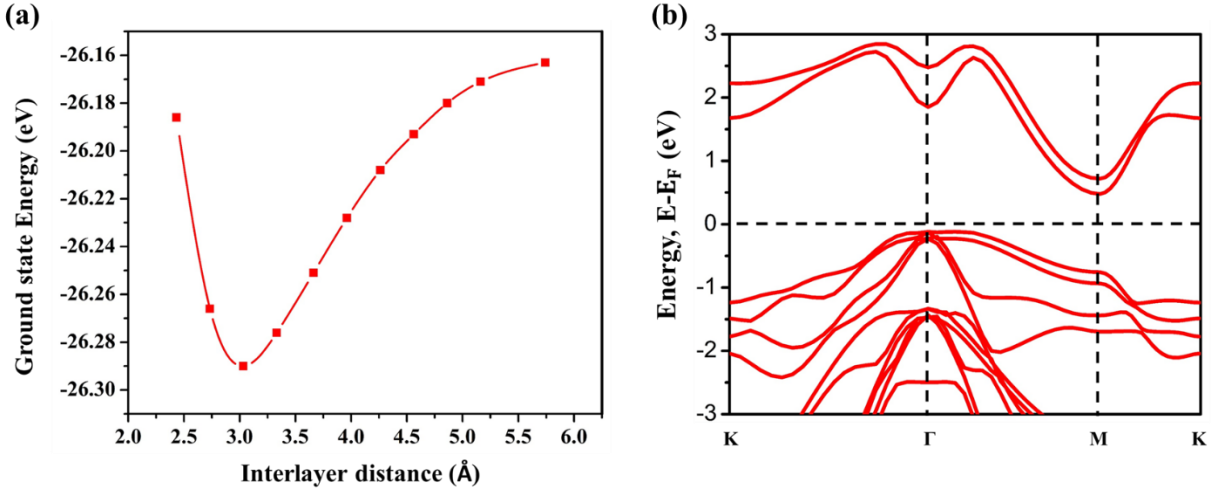


Fig. S6. Janus GeSSe bilayer (a) energy minimization with respect to interlayer distance and (b) electronic band structure.

6.2 Elastic properties:

Table S4. Calculated parameters for 2D Janus GeSSe monolayer and different stacking sequence of bilayer structure: in-plane elastic stiffness coefficient, C_{11} (N/m), C_{12} (N/m) and C_{22} (N/m); Young's modulus, Y_{2D} (N/m); shear modulus, G_{2D} (N/m) and Poisson's ratio, ν_{2D} . Born Huang (BH) mechanical stability criteria

Janus GeSSe	Stacking	C_{11}	C_{12}	C_{22}	Y_{2D}	G_{2D}	ν_{2D}	BH stability
Monolayer	-	77.15	22.39	77.15	70.65	27.38	0.29	yes
Bilayer	I	120.29	68.80	120.29	80.94	25.74	0.57	yes
	II	121.52	64.92	121.52	86.83	28.30	0.53	yes
	III	125.72	77.33	125.71	78.15	24.19	0.61	yes

In order to establish the mechanical stability of Janus GeSSe bilayer stacking sequences, Born-Huang (BH) elastic stability criteria for the trigonal crystal system has been verified, i.e. C_{11} ($= C_{22}$) > 0 , and $(C_{11} - C_{12}) > 0$. Therefore, the bilayer stacking sequences I, II and III are mechanically stable.

6.3 Born Effective Charges (BEC):

Monolayer	3.537	2.91	4.09	0.15	0.59	7.90	0.75
Bi-layer	3.525	8.96	73.26	0.07	0.29	604.34	0.60
Tri-layer	3.525	14.99	14.50	0.11	1.11	31.72	0.30
Tetra-layer	3.525	21.02	11.92	0.07	2.87	22.69	0.29
Multilayer	3.527	infinite	7.09	0.86	2.04	2.89	0.68

9. Thermal Properties

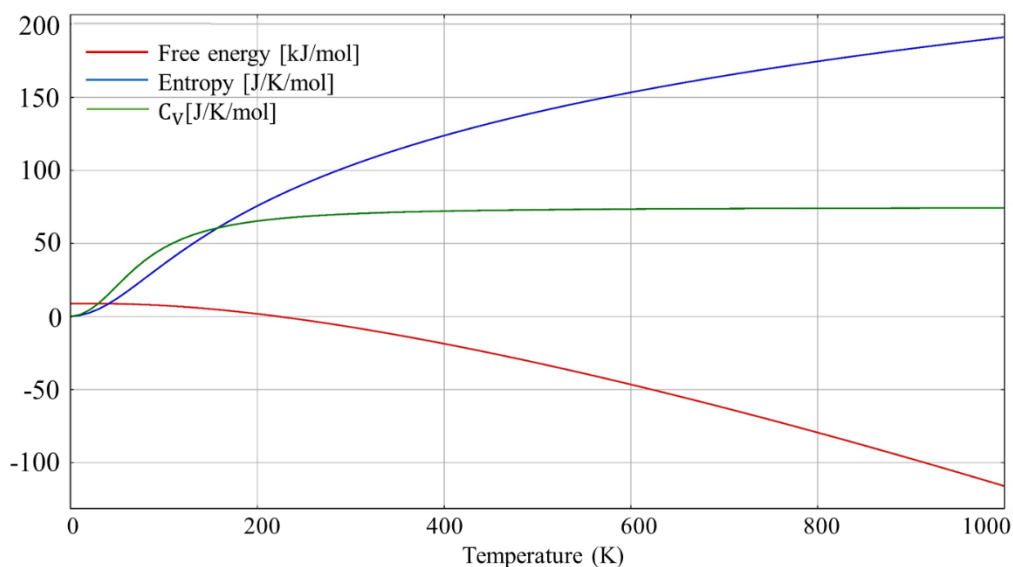


Fig. S7. Variation free energy, entropy and specific heat at constant volume (C_V) with respect to temperature for Janus GeSSe monolayer.

Reference

- 1 Dimple, N. Jena, A. Rawat, R. Ahammed, M. K. Mohanta and A. De Sarkar, *J. Mater. Chem. A*, 2018, **6**, 24885–24898.
- 2 S.-D. Guo and X.-S. Guo, *Phys. Chem. Chem. Phys.*, 2019, **21**, 24620–24628.
- 3 V. Zólyomi, N. D. Drummond and V. I. Fal'Ko, *Phys. Rev. B*, 2014, **89**, 205416.